Arch. Metall. Mater. **70** (2025), 2, 829-842

DOI: https://doi.org/10.24425/amm.2025.153485

ZHIXIN WANG[1*], JIANGTAO LI[1], MENGJIE PEI[1], MINGXING MA[2], XIAOZHE CHENG[1], QIAN ZHANG[1], XIAOYAN GUAN[1], HUILI DING[1], SHAOPEI JIA[1], QISONG LI[1], QUAN HUANG[1*]

MICROSTRUCTURES AND MECHANICAL PROPERTIES OF DIFFERENT MASS FRACTIONS OF Ti-COATED DIAMOND/ FeNiCrCuAl HIGH ENTROPY ALLOY COMPOSITES PREPARED BY SPARK PLASMA SINTERING

FeNiCrCuAl high-entropy alloy (HEA)/Ti-coated diamond composites were prepared by spark plasma sintering (SPS). The TiC coating was formed in situ on the surface of the diamonds through a vacuum micro-evaporation process. This study investigated the effects of varying mass fractions of diamonds (3 wt.%, 5 wt.%, 7 wt.%, and 12 wt.%) on the microstructure, microhardness, flexural strength, and wear properties of the high-entropy alloy. The results indicate that the TiC coating on the diamond surface effectively preserves the morphological integrity of the diamond within the FeNiCrCuAl HEA at an ambient temperature of 1000°C. Following sintering, the microstructure of the FeNiCrCuAl high-entropy alloy powder occurs transitions from a body-centered cubic (BCC) phase to a face-centered cubic (FCC) phase. As the mass fraction of diamonds increases, the hardness of the composites gradually increases. The composite containing 12 wt.% diamonds exhibits the highest hardness of 500.2 $HV_{0.5}$ within the FeNiCrCuAl HEA matrix, which is approximately 15.7% greater than that of the composite without diamond addition. Conversely, the flexural strength decreases with the increase of the heterogeneous interfaces created by the diamonds in the composites. The flexural strength of the composite containing 12 wt.% diamonds is only 277.0 MPa, representing a 51.6% reduction compared to the FeNiCrCuAl HEA. The composite compared with 7 wt.% diamonds demonstrates the best wear resistance, with an average friction coefficient of 0.16.

Keywords: High-entropy alloys; Ti-coated diamond; Composites; Microstructures; Mechanical properties; Interface bonding; Solid – solution strengthening

1. Introduction

Different from other traditional alloys which are composed of only one or two main elements, high-entropy alloys (HEAs) are made up of five or more elements within equimolar or near-equimolar ratios. The multiple major components make HEAs have a large mixing entropy (more than 1.5R, R is the universal gas constant) [1], which is more conducive to the formation of solid solutions with simple structures. By changing or increasing the alloying elements of HEAs, the microstructures and properties of HEAs can be adjusted to possess excellent high-temperature resistance, corrosion resistance, and other mechanical properties to match the service environment [2-4]. For example, for the high-entropy alloy composed of elements such as Fe, Co, Ni, Cr, etc. the addition of Ti element can increase the degree of subcooling during the solidification of HEAs and increase the nucleation rate of the liquid phase [5]. The addition of Al element can promote the formation of BCC phase, which can induce the transformation of alloy organization from FCC phase to BCC phase [6]. The addition of Cu element can lead to elemental segregation, and form Cu-rich and Ni-rich FCC solid solution phases in the region of inter-dendrite, which can result in the formation of FCC solid solution phase [7]. The addition of Mo element promotes the formation of intermetallic compounds in HEAs organization [8]. In addition, there are severe lattice distortions and slow diffusion effects exist in HEAs, resulting in grain boundary strengthening, dislocation strengthening, and solid solution strengthening [1,9,10], which gives HEAs better hardness and wear resistance [11,12]. The properties of excellent wear resistance, high toughness, and better hardness make HEAs a broad application prospect in the wear-resistant materials domain.

A series of studies have reported that HEAs can be used as matrix material in rigid grinding tools such as WC, SiC, and TiC, but the current research reports on HEA/diamond composites are still insufficient. For metal matrix diamond composites, the

[1] SCHOOL OF MATERIALS ELECTRONICS AND ENERGY STORAGE, ZHONGYUAN UNIVERSITY OF TECHNOLOGY, ZHENGZHOU, 451191, PR CHINA
[2] SCHOOL OF MECHANICAL ENGINEERING, HENAN POLYTECHNIC INSTITUTE, NANYANG, 47300, PR CHINA
* Corresponding author: zxwang72@163.com

retention capacity of the metal matrix for diamond particles needs to be improved to enhance grinding performance [13]. Traditional metal matrix diamond composites are prepared by mixing single metal or pre-alloyed powders with diamond particles through hot-press sintering. During this process, thermal is generated through the electric resistance wire heats up, and the heating rate is relatively slow. The low sintering temperature induces a mass of voids inside the sintered samples. It is easy to form defects such as intermetallic compounds, interstitial phases, or other deleterious phases, affecting the diamond particles' structural stability [14]. The phase composition of HEAs mainly consists of simple solid solutions, which exhibit excellent hardness and wear resistance. Replacing traditional metal binders to prepare HEA/diamond composites presents a vast space to explore. The interfacial bonding and strengthening behavior between diamond particles and HEA skeleton are still unclear.

In previous studies, the research direction for diamond-reinforced HEA composites primarily focuses on preparing HEAs coatings on the surface of target materials (such as #45 steel) through laser cladding [15-18], which exhibits high hardness and wear resistance. However, the diffusion of the metal matrix into the surface coating may change the alloy composition of the coating. Additionally, the relatively thin thickness of the coating on the matrix surface limits the potential application of HEA / diamond composites. Relatively, spark plasma sintering (SPS) completes the preparation of samples at a lower temperature utilizing solid-phase sintering, reduces the diffusion of carbon atoms into the HEA matrix, and makes the diamond particles distribute more uniformly. In the previous studies, Zhang [19] et al. prepared FeCoCrNi HEA by laser cladding and added diamond particles with a particle size of less than 75 μm as the reinforcement phase at different mass fractions (3, 6, 12 wt.%). With the increase of the diamond mass fraction, the hardness of the HEA coating increased at first and then decreased, and the wear depth and wear rate decreased first and then increased. The HEA coating containing 6 wt.% diamond has a good combination of wear resistance and hardness performance. Zhang [20] prepared FeCoCrNiMo HEAs/diamond composites through SPS with a diamond particle size of 200 μm. The composites prepared at 950°C and 30 MPa exhibited an excellent combination of mechanical properties, with a hardness of 630 HV and a transverse fracture strength of 1310 MPa, as well as an optimal wear resistance. The interfacial bonding strength between HEAs and diamond is a key factor affecting the retention ability and further affects the wear resistance and fracture toughness of the composite materials. There have been some studies on the interfacial bonding between diamonds and HEAs. However, the interfacial reaction and strengthening behavior between coated diamonds and HEAs are still unclear.

FeNiCrCuAl HEA exhibits excellent high-temperature stability and corrosion resistance, and the FCC and BCC dual-phase structure in microstructure endows HEAs with superior mechanical properties FeNiCrCuAl HEA can form a variety of metal oxides in a high-temperature environment due to its unique alloy composition, which renders it good high-temperature stability and corrosion resistance. In this work, diamond as a reinforcing phase was added into FeNiCrCuAl HEA to further enhance the hardness and wear resistance. Add a titanium coating to the diamond surface by vacuum evaporation coating process, the interfacial reaction between FeNiCrCuAl HEA and coated diamond was investigated. The aim is to make a preliminary exploration for the application of FeNiCrCuAl HEA in diamond composites, and exploit the application of HEAs in diamond tools.

2. Materials and methods

2.1. Materials Characterization Materials preparation and characterization

HEA powder with a nominal composition of $Fe_{20}Ni_{20}Cr_{20}Cu_{20}Al_{20}$ (in atomic percentage, the pure metal powders of Fe, Ni, Cr, Cu, and Al with purity higher than 99.99 wt.% by gas atomization, and the alloy powder particle size is 35-70 μm) was used as the metal matrix. The microstructures of HEAs powders can be seen in Fig. 1(a); the average size of most FeNiCrCuAl HEA powders is about 60 μm. Fig. 1(b) illustrates the XRD pattern of FeNiCrCuAl HEA powder prepared by gas atomization, which has good crystallization properties, and the phase structure is mainly a single BCC solid-solution phase.

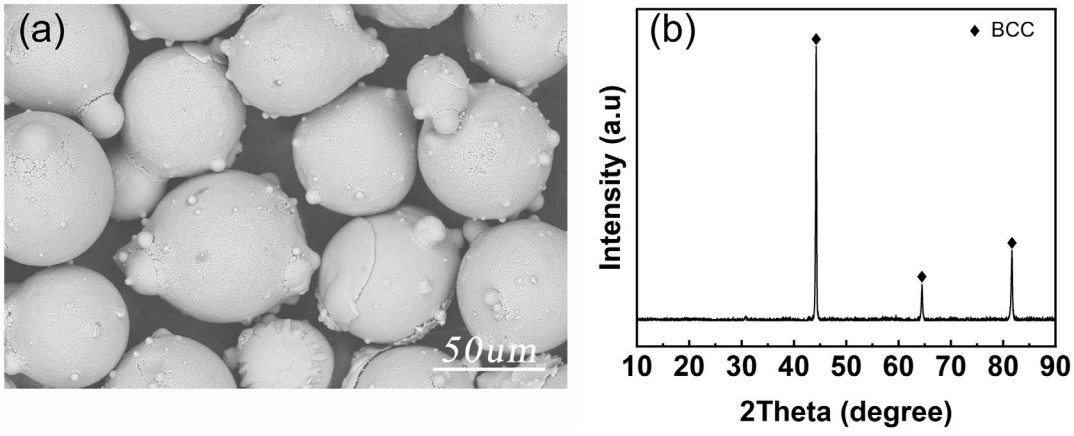

Fig. 1. SEM image of FeNiCrCuAl HEA powder (a); XRD pattern of FeNiCrCuAl HEA powder (b)

Ti coatings were applied to the surface of standard HWD5 synthetic diamond (average particle size is 70-80 mesh, provided by the Yellow River Cyclone), prepared using a vacuum micro-evaporation coating process, as illustrated in Fig. 3. The metal powder of Ti with a purity exceeding 99.99%, was initially mixed with a hydrochloric acid-ethanol solution to activate the metal powders for the preparation of the coating powder. Subsequently, the diamond particles were thoroughly combined with the coating powder (the mass ratio is 5:1) in a corundum mortar. The resulting mixed powder was then loaded into a graphite crucible for the coating process. A layer of the coated powder, approximately 2-3 mm in thickness, was applied to both the upper and lower surfaces of the diamond particle mixture to establish a coating atmosphere for the diamond particles under high-temperature conditions. The coating was conducted in a vacuum environment at a temperature of 850°C, with a holding time of 2 hours. As shown in Fig. 3(a), most of the diamonds exhibited smooth surfaces and particle shapes. The coating on the surface of diamond was damaged by short-term ball milling. It was measured that a titanium coating with a thickness of approximately 0.61 micrometers was formed on the surface of the diamond after the coating process, as shown in Fig. 3(c). TABLE 1 and Fig. 3(d) illustrate the spot canning element distribution results of spectrum1, the presence of titanium element was indeed detected in the coating on the diamond surface. The atomic percentage of titanium element to carbon element is approximately 1:5.

TABLE 1

Results of Spot Scanning Element Distribution

Element	Weight percentage	Atomic percentage
C	34.17	51.49
O	31.38	35.49
Ti	34.45	13.02

The X-ray diffraction (XRD) scanning pattern of Ti-coated diamond is illustrated in Fig. 3(b). In addition to the high-

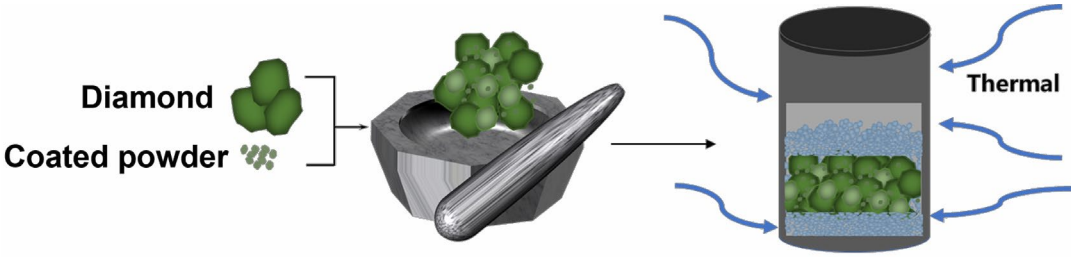

Fig. 2. Schematic diagram of the vacuum micro-evaporation coating process flow for diamond particles

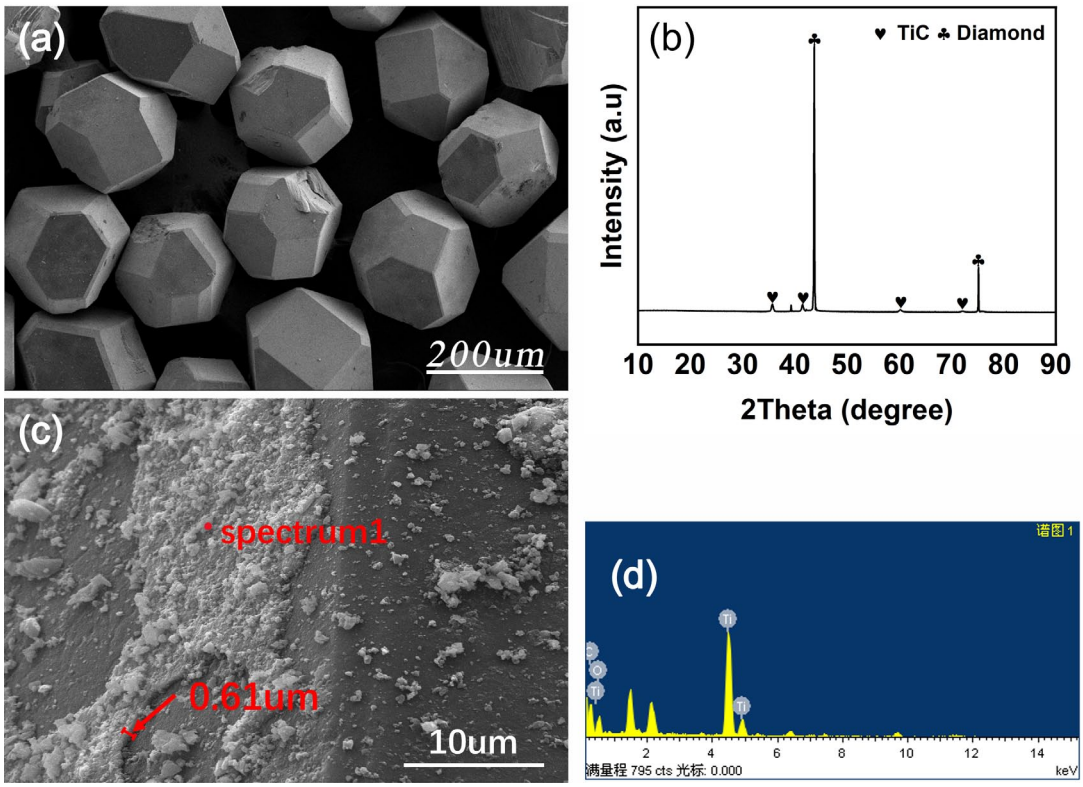

Fig. 3. SEM image of Ti-coated diamond (a); XRD pattern of Ti-coated diamond (b); magnified SEM image of Ti-coated diamond after ball milling 1 hour (c); Spot Scanning Element Distribution pattern of spectrum1 (d)

intensity peaks of the diamond phase, which were detected at the positions of 43.9° and 75.3°, the subdominant peaks of TiC were detected at the positions of 35.9° and 41.8°. This result demonstrated that the vacuum micro-evaporation coating process at 850°C formed a thicker TiC coating adhered to the diamond surface, which was generated by the close contact between Ti powder and the diamond surface under low pressure and a titanium vapour atmosphere during the coating process.

2.2. Preparation of FeNiCrCuAl HEA/diamond composite

Diamond particles are characterized by high hardness and high wear resistance. The free carbon atoms generated by decomposition at high temperatures can play a role in dispersion strengthening the HEA alloy matrix. However, the addition of diamond particles also introduces heterogeneous interfaces into HEA, reducing the toughness and ductility of HEA. Referring to the amount of diamond added in previous studies [13,19,20], it is determined to add 3 wt.%, 5 wt.%, 7 wt.%, and 12 wt.% diamond particles to FeNiCrCuAl HEA to prepare composites, which were designated D3, D5, D7, and D12, respectively. The powders of HEAs and diamonds were further mixed by wet ball milling using a planetary ball mill to achieve a uniform distribution of diamonds inside FeNiCrCuAl HEA powder. Anhydrous ethanol was employed as the solvent for wet ball milling, with a ball-to-powder mass ratio of 10:1, a milling speed of 300 rpm, and a mixing time of 3 h. The completed mixed (FeNiCrCuAl) C_X (x = 3 wt.%, 5 wt.%, 7 wt.%, 12 wt.%) powder was subsequently dried in a vacuum drying oven at 80°C for 5 h. The dried powder was put into a graphite mold with a diameter of 25 mm and heated to 1000°C using an SPS furnace (SPS-30, Chenxin Weike Industrial Technology Co. Ltd., Ningbo). When using SPS for the solid-phase sintering of alloy powders, if the temperature is too high, excessive liquid metal will form in the graphite mold. This can cause the metal to seep out of the graphite mold, affecting the composition and dimensions of the metal sample. The seepage of metal elements that can react with carbon elements will also damage the graphite mold [21]. When the temperature is too low, it will affect the metallurgical bonding between the metal powders. In our previous experiments, FeNiCrCuAl HEA powders were sintered at 900℃, 1000℃, and 1100℃ respectively. Comparing the specific situations and mechanical properties of the samples prepared at the above temperatures, the temperature of 1000℃ is more suitable for the sample preparation in this work. The parameters of the sintering process were optimized to be pressure 30 MPa. During the initial heating phase, when the heating temperature was below 600°C, the heating rate was 100°C/min. From 600°C to 900°C, the heating rate was reduced to 50°C/min. From 900°C to 1000°C, the heating rate was 25°C/min, holding the sintering temperature of 1000°C for 8 minutes. Preserve a negative pressure inside the furnace and allow it to cool naturally to room temperature.

2.3. Microstructure and property characterization

The graphite layer absorbed on the surface of FeNiCrCuAl HEA/diamond composites caused by the appliance of graphite molds during the sintering process was removed using 400#, 600#, 800#, and 1000# SiC sandpaper. Subsequently, the surfaces of the samples were further polished with 2000 mesh diamond polishing discs. Sample strips for flexural testing were cut from 25 mm diameter samples using a DK7735 CNC wire cutter. The longitudinal sections of the sample strips were smoothed to prevent fractures caused by stress concentration resulting from the irregular surface morphology of the samples. The composition of the samples was analyzed using the Ultima IV multifunctional X-ray diffractometer from Japan through Cu Kα diffraction lines. The scanning speed was set at 10°/min, with a step speed of 0.2°/min, the scanning range was from 10° to 90°, the operating voltage was 40 kV, and the working current was 20 mA. A ZEISS Gemini SEM 360 field emission scanning electron microscope equipped with an energy dispersive spectrometer (EDS) was utilized to investigate the microstructure and elemental distribution of the samples. The hardness of the metal matrix within the composite materials was assessed using the HVS-1000 Vickers microhardness tester, with an applied load of 500 g and a testing duration of 15 seconds. To minimize errors attributable to human factors during the measurement process, hardness measurements were conducted within a 500 μm range around the diamond particles, and the average value was calculated from multiple measurements taken in each test area. The flexural performance of the samples was evaluated through the three-point bending method, utilizing an Instron 3369 universal testing equipment to measure samples with a height-to-width ratio of 1.5:1 and a pivot span of 9 mm. Friction and wear tests were conducted using reciprocating friction and wear tester (MFT-R4000), with a test load of 30 N, a sliding speed of 3 m/min, and a test time of 30 min. Take measurements multiple times in different regions on the surface of the same sample and then calculate the average value. Si_3N_4 ceramic balls (φ = 6 mm) were employed as friction partners. The wear areas of the friction surfaces of the Si_3N_4 ceramic balls were quantified after the friction and wear tests.

3. Results and discussions

3.1. Microstructure and phase analysis

Fig. 4 shows the XRD patterns of FeNiCrCuAl HEA/diamond composites with different mass fractions of Ti-coated diamond. FeNiCrCuAl HEA as the metal matrix constituent of the composites, prepared by SPS has both FCC and BCC dual-phase structures [22]. Notably, the XRD pattern of the sintered samples reveals the emergence of the FCC phase peak, which differs from that of the raw material. With the increase of diamond mass fraction inside the composites, the dominated and subdominant diffraction peaks of diamond appear at diffraction angles of 43.9° and 75.3°, respectively. Moreover, the half-height

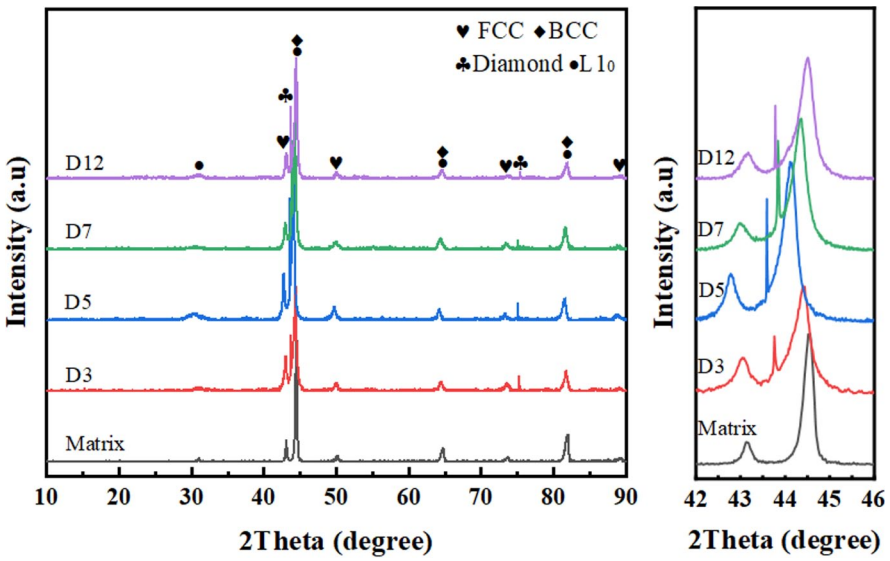

Fig. 4. XRD pattern of FeNiCrCuAl /Ti-coated diamond composites

width of the diamond diffraction peaks in each sample doesn't appear broadening phenomenon, which indicates that the diamond in each sample has not undergone significant structural changes, and no graphite peaks were observed in the XRD patterns. Cr is a strong carbide-forming element that can react with the C elements present in the FeNiCrCuAl HEA matrix to form carbides such as Cr_7C_3. However, with the increase of the mass fraction of diamond in the composites, there are no obvious carbide peaks observed in the XRD patterns. This demonstrates that there is either no or only a negligible quantity of carbon incorporated into the FeNiCrCuAl HEA matrix. In addition, it also substantiates the diffusion-blocking effect caused by the TiC coating effectively regulates the diffusion of carbon elements from the diamond surface into the FeNiCrCuAl HEA matrix. The XRD patterns of all samples exhibit the presence of FCC phases enriched in Al and Ni elements, which were identified as an intermetallic compound with the $L1_0$ structure, based on the synthesis and conclusions of previous studies on HEAs containing Al and Ni elements [23,24]. When the addition of diamond exceeded 5 wt.% in the composites, the $L1_0$ phase exhibited a diffraction peak with a gentle shape at a diffraction angle of 30.9°. The XRD patterns revealed different degrees of shifts toward the lower angle, with the overall maximum shift reaching approximately 0.2°. The solid solution of Ti atoms, which have a larger atomic radius, adhered to the surface of Ti-coated diamond and diffused into the FeNiCrCuAl HEA matrix, resulting in lattice distortion. This distortion led to an increase in the lattice constant of the FeNiCrCuAl HEA solid solution. The substituted atoms facilitated the formation of intermetallic compounds with small particle sizes that diffused into the FeNiCrCuAl HEA matrix. All of these factors contributed to the lower angle excursion of the diffraction peaks.

Fig. 5(a) illustrates the scanning electron microscopy (SEM) micrographs and energy-dispersive X-ray spectroscopy (EDS) mappings of the bonding interface between diamond particles and the FeNiCrCuAl HEA. A Cr-rich transition layer with a thickness of approximately 6 μm was observed at the interface between the diamond and HEA matrix in the FeNiCrCuAl HEA/diamond composites prepared by SPS. Additionally, the TiC coating absorbed on the surface of the diamond allowed it to maintain a complete grain structure following sintering. The EDS results indicated that no obvious carbon diffusion phenomenon existed in the vicinity of the diamond particles within the FeNiCrCuAl HEA matrix. The vacuum micro-evaporation coating process facilitated the in-situ uniform and continuous growth of the TiC coating on the diamond surface. This coating effectively hinders direct contact between Fe, Co, Ni, and other metallic elements that promote graphitization with the diamond particles [25], which is particularly effective when diamond particles are exposed to high temperatures. Otherwise, the coating hinders the diffusion of free carbon atoms into the FeNiCrCuAl HEA matrix. Fig. 5(a) illustrates the presence of an enriched region of Cr surrounding diamond particles, which is formed as C atoms penetrate the TiC coating and attract Cr atoms from the FeNiCrCuAl HEA matrix. The thin TiC coating is insufficient to entirely impede the diffusion of free carbon atoms generated from the diamond surface at high temperatures.

Fig. 5(b) is a magnified image of the area within the yellow dashed-line frame. In the bonding region between the Ti-coated diamond and the FeNiCrCuAl HEA, there is a transition layer rich in titanium elements filling the gaps existing between the diamond and the HEA matrix. The presence of the titanium transition layer changes the bonding mode between the diamond and the HEA matrix from mechanical interlocking to a more robust metallurgical bonding. The result of the line scanning element distribution shows the distribution intensity of titanium and carbon elements with the change of distance from the Ti-coated diamond particles to the FeNiCrCuAl HEA matrix. It can be seen that the thickness of the titanium transition layer on the diamond surface is close to 1um. Moreover, the concentration of carbon elements in the diamond/FeNiCrCuAl HEA composite material drops rapidly after passing through the titanium transition layer,

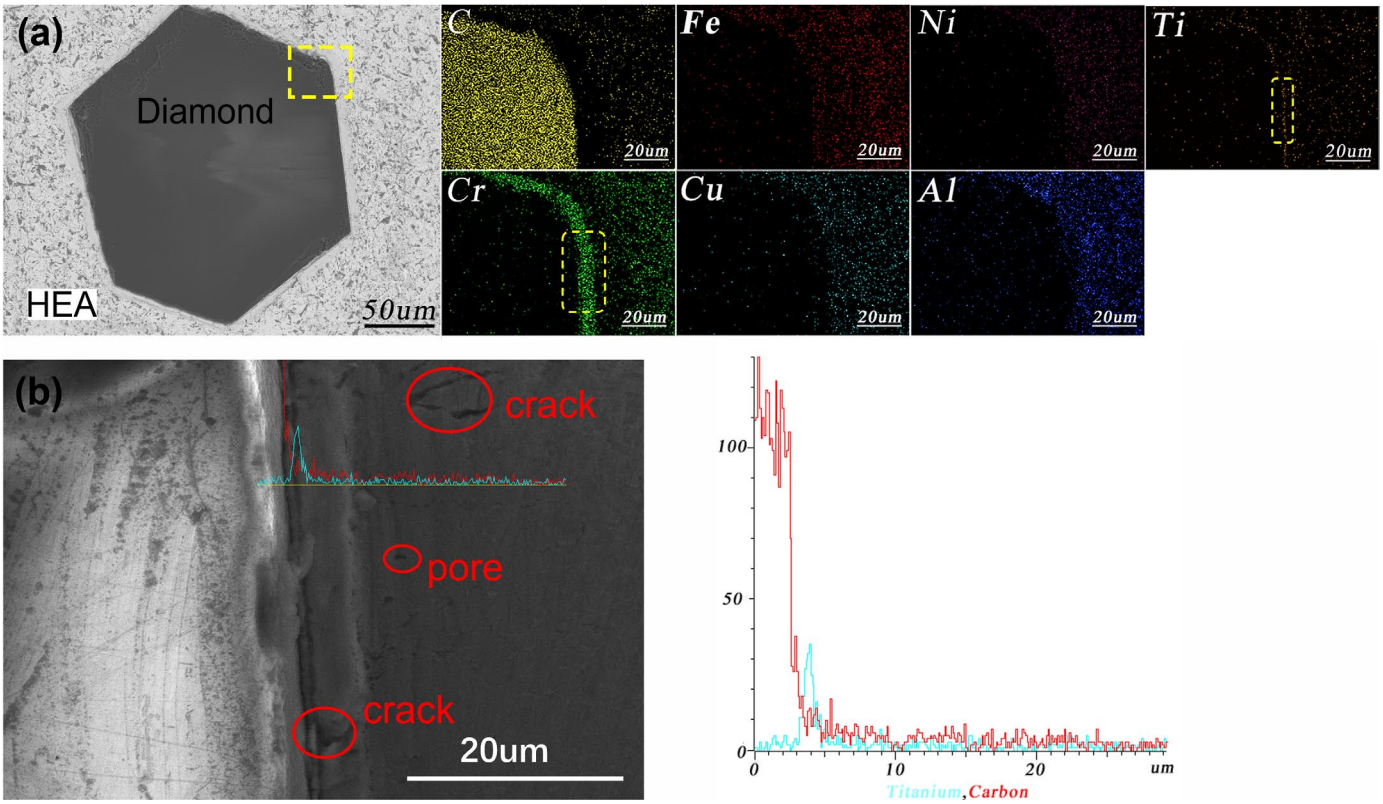

Fig. 5. SEM micrographs and EDS mappings of Ti-coated diamond/HEA composite (a); magnified image of the area within the yellow dashed-line frame and Line – scan elemental distribution spectrum (b)

which proves that the titanium coating on the diamond surface effectively hinders the diffusion of carbon atoms on the diamond surface into the HEA matrix. Titanium elements mainly exist in the coating on the diamond surface, and there is a small amount of diffusion of titanium atoms into the FeNiCrCuAl HEA matrix. In the HEA matrix adjacent to the diamond particles, the presence of micro-cracks and voids is clearly observed. The formation of these defects is most likely attributed to the following factors: The brittle carbides and intermetallic compound contained in the HEA matrix significantly reduce the tensile strength of the alloy structure, making it extremely likely to be the starting point of cracks [26,27]. As shown in Fig. 5(b), within the Cr-enriched region, a crack can be clearly seen running through the entire chromium transition layer. The significant differences in the diffusion rates of different types of metal atoms lead to the aggregation of vacancies at the interface, thus forming voids. Taking the Cu/Ni diffusion couple as an example, since the diffusion rate of Cu atoms is significantly faster than that of Ni atoms, voids appear in the regions where Cu elements are concentrated [28]. Inadequate or improperly set process parameters (including temperature, pressure, and time) prevent the interface from achieving complete metallurgical bonding, which also results in the retention of micro-pores in the alloy structure [29]. The oxides, grease, as well as adsorbed gases (such as O_2, N_2, etc.) adhering to the surface of diamond, impede the metallurgical bonding process between metal atoms, ultimately resulting in the formation of cracks or voids within the alloy structure. Optimizing the sintering process parameters of the FeNiCrCuAl HEA powder, promoting the flow of liquid metal between the HEA powders, and enhancing the metallurgical bonding between the HEA powders can reduce the presence of defects such as micro-cracks and voids, enabling the FeNiCrCuAl HEA matrix to achieve higher strength.

The SEM micrographs demonstrate the presence of Cr-rich areas in the bonding region between the diamond and FeNiCrCuAl HEA matrix. In addition, there is almost no diffusion of other alloying elements in HEAs matrix spread to diamond interface in this region. The multi-layer structure of TiC and Cr-rich layers in the transition region between diamond and HEAs matrix is the primary factor ensuring diamond particles maintain complete crystal morphology. The EDS patterns indicate the presence of tiny amounts of Ti element on the surface of diamond particles, which exhibits a decreasing gradient as they diffuse into FeNiCrCuAl HEA matrix. The Ti atoms with larger atomic radius diffused into FeNiCrCuAl HEA matrix to form a substitution solid solution, thereby enhancing the strength of metal skeleton composed of HEAs in the region adjacent to diamond particles. Ti-coated layer on the surface of diamond formed a TiC coating by diffusion to the surface of diamond and substitution solid solutions by diffusion to FeNiCrCuAl HEA matrix, respectively. Ti-coated layer filled the gap formed by the semi-coherent boundary connection between diamond and HEA matrix caused by the difference in lattice types [30,31]. This results in a closer metallurgical bonding between diamond particles and FeNiCrCuAl HEA matrix, meanwhile enhancing the retention force of HEAs matrix to diamond particles.

The diamond particles in HEAs composed of Fe, Co, Ni, and other graphitization elements can retain a slight graphitized state due to the characteristics of the SPS process. Powerful covalent bonds exist between the carbon atoms on the surface of the diamond, so intense activation energy is required to break bondage from the diamond interface and form freely diffusing carbon atoms [32]. The SPS process utilizes plasma generated by high current and low voltage during the powder sintering process to heat the sample powders, achieving the desired temperature for sample preparation in a relatively short period. This process induces rapid melting of the surface of the pre-alloyed spherical powder, forming connections between particles to create bulk samples. Besides, the sintering temperature of the samples can be precisely regulated, enabling the preparation process to be completed at a temperature inferior to the casting temperature. This point mitigates the adverse effects of elevated temperatures on the transformation of diamond into graphite or the amorphous phase, thereby preserving the integrity of the diamond particles. Furthermore, applying uniaxial pressure during the solid-phase sintering process facilitates the fabrication of high-density samples from alloy powder. This approach reduces the void ratio in the samples while simultaneously lowering the sintering temperature, facilitating the preparation of HEA/diamond composites with high-density and intact diamond particles.

3.2. Mechanical properties of HEA/diamond composites

3.2.1. Hardness and bending strength

Due to the difference in density between diamond and FeNiCrCuAl HEA (the density of diamond is 3.52 g/cm^3, and the theoretical density of FeNiCrCuAl HEA based on the mass fractions of its constituent elements is 7.85 g/cm^3), diamond with lower density added into HEAs matrix will lead to HEAs/diamond composite with a lower density than that of the FeNiCrCuAl HEA. Fig. 6 illustrates the density of the FeNiCrCuAl HEA prepared by SPS is 7.25 g/cm³ determined by Archimedes' drainage method [33]. The expressions for specific gravity and density are as follows [33],

$$SG = \frac{W_a}{W_a - W_w} \tag{1}$$

$$Density\ of\ specimen = \frac{SG}{\rho_L} \tag{2}$$

where W_a is mass of specimen in air, W_w is mass of specimen in water, SG is specimen gravity of the immersing liquid in a consistent unit, ρ_L is density of the water (997.6 kg/m^3). The density of the composites gradually decreased with the increase of diamonds added into HEAs. When the mass fraction of diamond reached 12 wt.%, the measured density of the composites was 6.44 g/cm³. In terms of the FeNiCrCuAl HEA/diamond composites, the hardness of the composite is primarily influenced by the mass fractions of diamond, considering that diamond possesses significantly higher hardness than HEAs. In contrast, the density of diamond is only half that of the FeNiCrCuAl HEA. The surface of the diamond can act as a solid-liquid interface during the solidification process, providing a nucleation and growth site for the solidification of liquid FeNiCrCuAl HEA. This facilitates the secondary growth of the FeNiCrCuAl HEA microstructure and results in significant refinement of the alloy structure around the diamond particles [34,35]. Moreover, the free carbon atoms diffuse from the diamond interface at high temperatures and dissolve into the HEAs, forming interstitial solid solutions. The strengthening effect caused by lattice distortion enhances the hardness of the FeNiCrCuAl HEA matrix. Part of the free carbon atoms diffuse into FeNiCrCuAl HEA and react with Cr present in the alloy composition, as well as Ti atoms diffuse from the diamond interface to form carbides. These carbides are dispersed within the HEAs matrix, further enhancing the hardness of the FeNiCrCuAl HEA matrix.

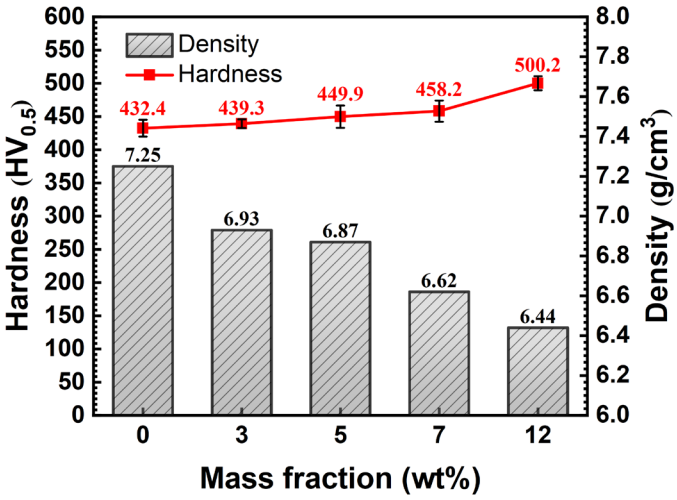

Fig. 6. Hardness and density of FeNiCrCuAl HEA/diamond composites prepared by SPS

TABLE 2

Comparison of the hardness of FeNiCrCuAl HEA with that of other metal-matrices used as diamond composites

Metal-Matrix	Sintering Temperature, °C	Hardness, HV
ODS $CuZn_{20}$	760	124
ODS iron powder	1000	234
Ultra-fine iron powder	700	164
Co powder	800	309
FeCoNiSnWC (2%TiH2+CeO2) [36]	780	309
FeCoCrNiMo [37]	1150	350-520
CoCrCuxFeNi [38]	1100	188-327
$Cr_5Cu_{20}Fe_{25}Mn_{25}Ni_{25}$ [39]	800	407-458
FeNiCrCuAl (this study)	1000	432

Note: ODS: oxide dispersion strengthened

TABLE 2 lists the hardness values of some metal matrices used in diamond tool materials. When compared with the hard-

ness of FeNiCrCuAl HEA used in this study, it can be seen that the hardness value of FeNiCrCuAl HEA is more than about 1.5 times higher than that of the metals commonly used in diamond tools. Moreover, compared with several HEAs listed in the table, decreased the use of Co metal, which is harmful to human health. The FeNiCrCuAl HEA has good high-temperature stability and corrosion resistance, expanding the application of HEAs in diamond tool materials. The lattice distortion induced by the substitution solid solution formed by Ti atom dissolved in the FeNiCrCuAl HEA also contributes to the reinforcement of the hardness of the HEAs matrix. As the diamond added to HEAs increased from 0 wt.% to 12 wt.%, the hardness of the HEAs matrix only increased from 432.4 $HV_{0.5}$ to 500.2 $HV_{0.5}$. This limited increase in hardness can be attributed to the constraints imposed by the diamond's surface transition layer on the diffusion of carbon atoms into the FeNiCrCuAl HEA matrix. Although the increase in diamond mass fraction positively affected the hardness of the FeNiCrCuAl HEA matrix, the trend of hardness improvement was relatively gentle. When the diamond mass fraction increased from 3 wt.% to 12 wt.%, the microhardness of the FeNiCrCuAl HEA matrix only increased by 14%. In previous experiments, Zhang [40] prepared $FeNiCoCrTi_{0.5}$ HEA/diamond composite coating materials by laser melting, using diamond particles with a particle size of 45 μm as the reinforcing phase. The microhardness of the $FeNiCoCrTi_{0.5}$ HEA coatings increased by about 2.5 times when the addition of diamond was increased from 3 wt.% to 12 wt.%. Significant differences were observed between the two experiments regarding the enhancement of microhardness in HEAs through the addition of diamonds. The main reasons for these differences can be attributed to the following two aspects: On the one hand, the smaller grain size of diamond provides more attachment surfaces for the solidification of HEAs, promoting the organization refinement of HEAs matrix [41]. Moreover, the distribution of diamond particles with smaller grain sizes in HEAs matrix is more uniform, which is more conducive to the sufficient diffusion of C atoms detached from the diamond surface into HEAs matrix. On the other hand, laser cladding provides a higher thermal input for the HEAs coating, which promotes the graphitization of diamond and contributes additional C atoms, thereby enhancing solution strengthening and carbide dispersion strengthening to improve the hardness of the HEAs matrix. SPS can achieve the sintering of samples at lower temperatures, and when combined with the TiC coating prepared in our study effectively mitigates the graphitization of diamond, allowing for the retention of a more complete morphology of the diamond particles.

Fig. 7(a) shows the three-point bending stress-strain curves of FeNiCrCuAl HEA/diamond composites. FeNiCrCuAl HEA exhibited excellent bending resistance with only a small amount of deformation occurring under the maximum load of 2000 N during the experiment, and the deformation reverted when the axial pressure was unloaded. Among the composites with different mass fractions of Ti-coated diamond, the composite containing 3 wt.% diamond exhibited the best flexural properties, experiencing a brittle fracture at a strain of 0.14% under uniaxial pressure of 470 MPa. Conversely, the composite with 12 wt.% Ti-coated diamond showed the worst flexural properties, with a brittle fracture occurring at a strain of 0.084% under uniaxial pressure of 366 MPa. Fig. 7(b) shows the flexural strength of FeNiCrCuAl HEA/diamond composites, which supplemented with different mass fractions of diamond decreased gradually with the increase of diamond mass fraction in the HEAs matrix. The reason might be attributed to the introduction of diamonds into the FeNiCrCuAl HEA, which creates additional heterogeneous interfaces to the internal organization of the composites. Due to the difference in the coefficient of thermal expansion between diamond and HEA, as illustrated in TABLE 3, deflection cracks pointing towards the diamond particles will occur in the HEA matrix around the Ti-coated diamond during solidification. When the diamond content is high, the overlapping of particles leads to a decrease in fracture toughness [42]. As the mass fraction of diamond increases, the area of these heterogeneous interfaces also increases, contributing to the reduction in bending resistance. The composite with 12 wt.% Ti-coated diamond showed the poorest bending resistance due to the internal multi-interface structure.

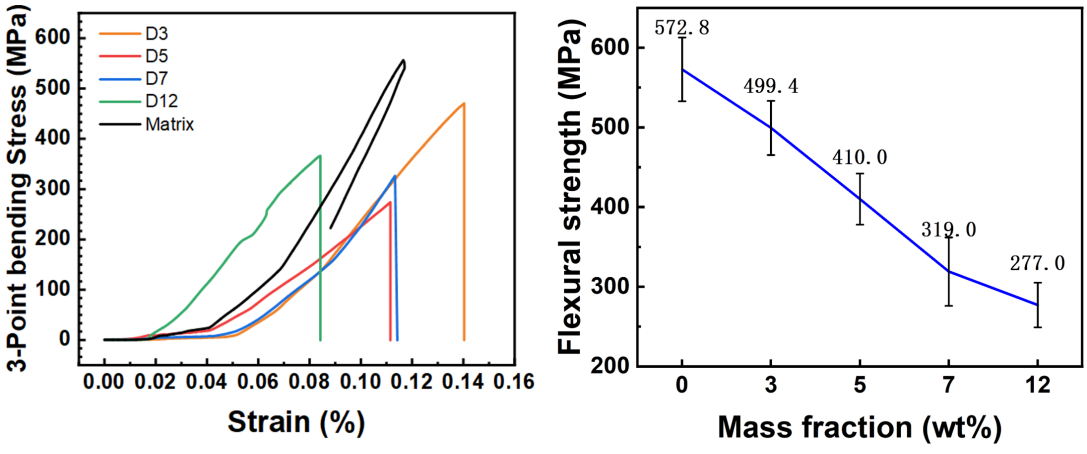

(a) (b)

Fig. 7. Three-point bending stress-strain curves of the HEA/diamond composites (a); Flexural strength of the HEA/diamond composites prepared by SPS (b)

TABLE 3

The atomic radius and thermal expansion coefficient of each element

Element	C	Fe	Ni	Cr	Cu	Al	Ti
Thermal expansivity (10^{-6}/°C)	0.8~1.1	11.8	13.4	4.9	16.5	23.1	8.6
Atomic radius (pm)	77	126	124	130	128	143	147

Fig. 8 shows the SEM micrographs and EDS mappings of the fracture surfaces belonging to the composites with 5 wt.% Ti-coated diamond. The scanning results of the elemental and the percentage of atomic distribution of the fracture surfaces are shown below. Fig. 8(a) shows the fracture surface of the FeNiCrCuAl HEA matrix. The relative atomic mass fraction of Al element reaches 53.52 at.%, indicating that the fracture surface of the FeNiCrCuAl HEA matrix is the Al element enriched region. Fig. 8(b) shows the fracture surfaces adjacent to the diamond particles. The relative atomic mass fraction of Al element is 33.80 at.%. In contrast, Cr atom near the diamond particles represents another enriched element, with a relative atomic mass fraction of 20.82 at.%. It can be inferred that the FeNiCrCuAl HEA/diamond composites are more likely to rupture at the region where Al-containing solid solutions or intermetallic compounds gathered in a relatively dense organizational surface. Corroborating the XRD results of Fig. 4, it can be confirmed that a significant amount of NiAl-rich intermetallic compounds exists in the Al-enriched region. The phase composition in the Cr-enriched region approached diamond particles primarily consists of BCC Cr-rich phases. The formation of numerous low-plasticity BCC solid solution phases and intermetallic compounds has increased the possibility of brittle fracture under high-stress conditions in this area. In addition, diamond particles retained in composites introduce heterogeneous interfaces in the composites. The diamond-TiC-HEA multilayer structure formed between the diamond and the FeNiCrCuAl HEA through a Ti-coated pretreatment of the diamond surface. This structure fills the gap between the diamond and the HEA, further weakening the insufficient bonding strength of the semi-coherent boundary between the diamond and the HEAs matrix [43]. However, compared to the bonding strength of the FeNiCrCuAl HEA matrix, the bonding strength between the diamond and the HEAs is still lower, and it is more likely to fracture at the diamond interface under high stress. The presence of BCC solid solution phases and intermetallic compounds on the surface of the diamond particles forms transition layers with a hard and brittle structure, aggravating the accumulation of stress around the diamond particles. Consequently, FeNiCrCuAl HEA/diamond composites are more inclined to brittle fracture at surfaces enriched with diamond particles. SEM observations of the fracture morphology of Ti-coated diamond composites reveal numerous fine, flaky tissue fragments on the fracture surface. The fractures in the FeNiCrCuAl HEA matrix and the fractures approaching the diamond particles confirm that the Ti-coated diamond composites exhibit brittle fracture characteristics.

3.2.2. Friction and Wear Properties

The classic forms of material wear failure are abrasive wear and adhesive wear [44]. In terms of the HEA/diamond composites, the primary reasons for wear failure are diamond particle spalling and matrix wear. Fig. 9(a) illustrates the experimental results of the friction coefficient for Ti-coated diamond composites and FeNiCrCuAl HEA. From the average friction coefficient curve, it can be inferred that the friction coefficient of FeNiCrCuAl HEA exhibits sluggish transitions and reaches the highest friction coefficient among the samples of 0.42. In contrast, the addition of diamond particles into FeNiCrCuAl HEA results in a significant decrease in the friction coefficient of the composites. The friction coefficient curve of Ti-coated

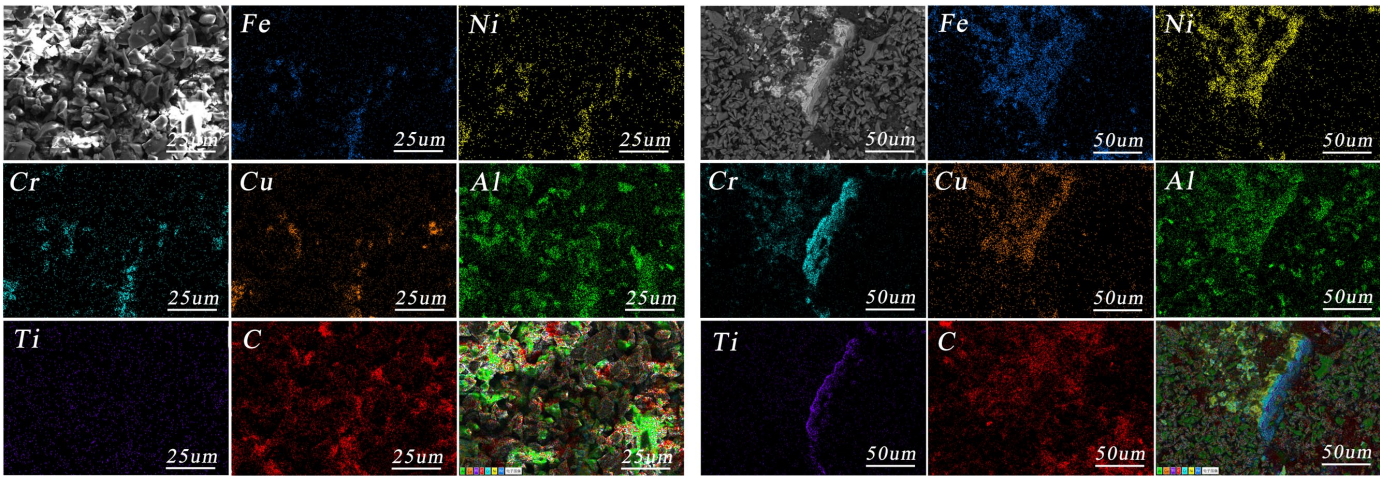

(a) (b)

Fig. 8. SEM and EDS patterns of the fracture surfaces of HEA matrix (a) and the region approached to the diamond particles (b)

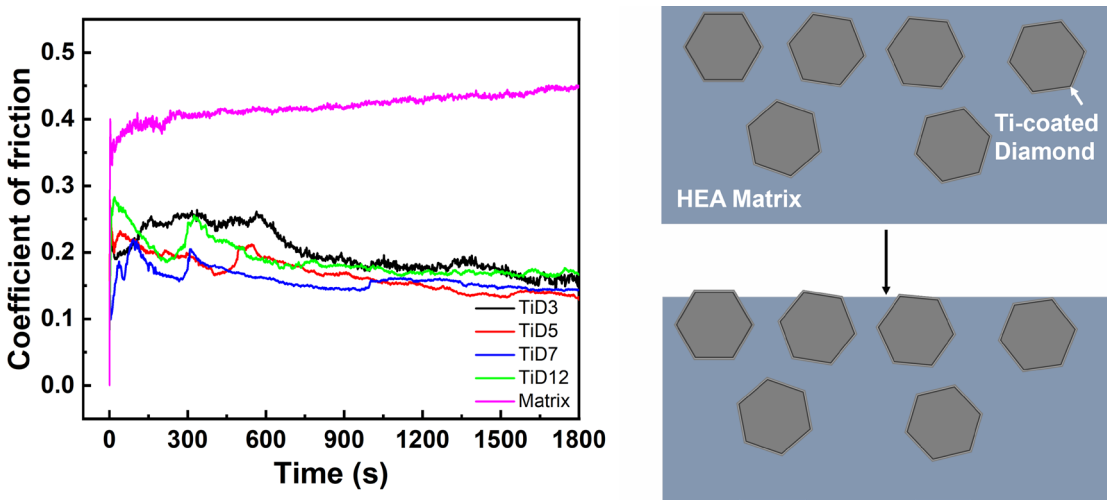

(a) (b)

Fig. 9. The friction coefficient-time curves of Ti-coated diamonds composites and HEA (a); Schematic Diagram of the Wear Process of Ti-coated Diamond/FeNiCrCuAl HEA Composites (b)

diamond composites tends to be stable after the initial stage of intense friction, characterized by considerable fluctuations for approximately 10 min. The final friction coefficient stabilizes between 0.15-0.20, indicating that the wear-resistant property of the composites has significantly improved compared with that of FeNiCrCuAl HEA. Among the Ti-coated diamond composites prepared during this experiment, the average friction coefficients of the D5 and D7 samples are close to each other, which are 0.17 and 0.16, respectively, which demonstrates the excellent wear resistance of these composites. In Zhang's research [45], a Ti/Ni coating was added to the surface of diamonds to prepare FeCoCrNiMo HEA/diamond composite materials. A low friction coefficient of 0.04 was obtained under a load of 50 N. The carbide layer on the surface of the diamonds ensures a stronger interfacial bonding ability and protects the diamond abrasive grains from excessive reaction with the base material. During the wear process of the Ti-coated diamond/FeNiCrCuAl HEA composite material, the HEA matrix on the surface of the sample is worn first. This continues until the diamond particles are exposed on the surface of the sample and start to participate in the wear process. The order of wear is HEA matrix- titanium coating-diamond particles, as shown in Fig. 9(b). The titanium coating maintains the complete particle morphology of the diamond, preserving its excellent cutting ability. However, at the same time, it also weakens the lubricating effect of the graphitization on the diamond surface [46]. The titanium coating enables a good metallurgical bonding to form between the diamond and the FeNiCrCuAl HEA matrix, as shown in Fig. 10, no fracture or detachment of the diamond particles was found on the surface of the worn sample. Therefore, the composite material sample after wear only experiences a minimal mass loss. In order to more intuitively represent the wear resistance of the composites containing different mass fractions of Ti-coated diamond, adopting the method to calculate the wear area of the Si_3N_4 ball friction pair used in the friction and wear experiments. TABLE 4 shows the increasing trend of the wear area of Si_3N_4 balls in relation to the average friction coefficient and mass loss of each composite material. The addition of diamond particles significantly improves the wear resistance of the HEA. The largest wear area of 0.80 mm², was observed for the Si_3N_4 ball in friction with the D7 sample, indicating that the D7 sample exhibits the best wear resistance.

TABLE 4

Abrasion area of Si_3N_4 balls, Average friction coefficient, and mass loss of Ti-coated diamond/FeNiCrCuAl HEA composites

Mass fraction	Wear area (mm^2)	Average friction coefficient	Mass loss (mg)
0 wt.%	0.24	0.42	2.35
3 wt.%	0.57	0.20	0.80
5 wt.%	0.63	0.17	0.30
7 wt.%	0.80	0.16	0.25
12 wt.%	0.67	0.19	0.12

Fig. 10 illustrates the abrasion morphology of Si_3N_4 balls and composites with different mass fractions of diamond. The wear morphology, reveals that the wear surfaces of Ti-coated diamond composites present elongated scratches, indicating that the primary abrasion pattern mechanism is abrasive wear. Additionally, partial areas are accompanied by flaky spalling, indicating that besides abrasive wear, there is adhesive wear in local regions during the wear process of Ti-coated diamond composites. But either obvious scratches or deformations aren't observed on the surface of the diamond particles in the wear morphology of the composites, indicating that the SPS process at a temperature of 1000°C doesn't form prominent graphite layers on the diamond surface. The wear mass of the composite material decreases with the increase of the mass fraction of diamond. There is no shedding of diamond particles on the worn surface, and the main form of wear is adhesive wear of the metal matrix. The TiC coating on the surface of the diamond particle prevents direct contact between the alloying elements of FeNiCrCuAl HEA and

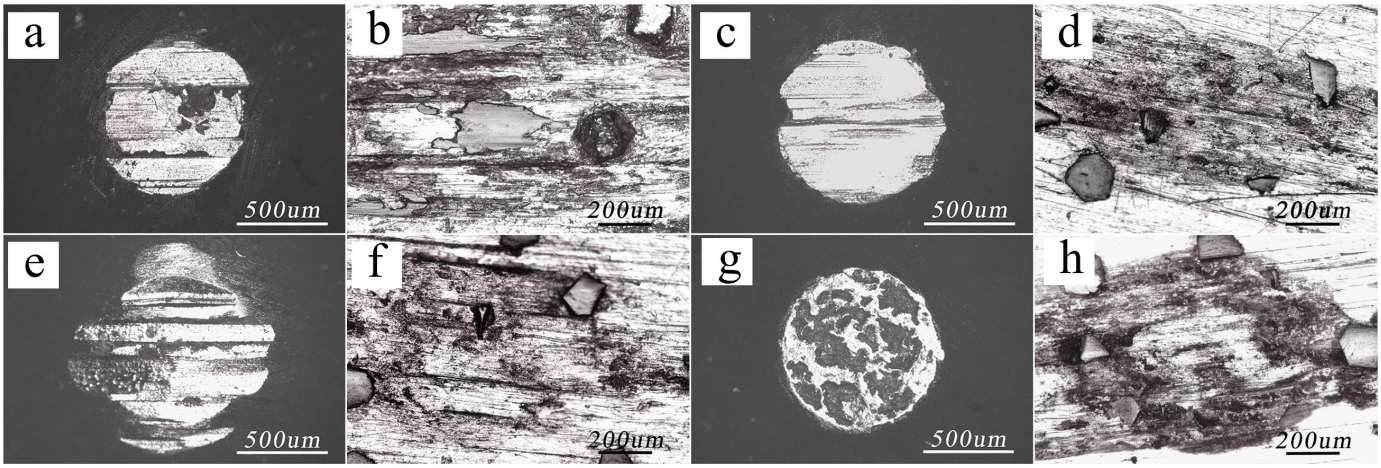

Fig. 10. The abrasion morphology of Si_3N_4 balls and composites with different mass fractions of diamond, 3 wt.% (a, b); 5 wt.% (c, d); 7 wt.% (e, f); 12 wt.% (g, h)

diamond surface. Consequently, the contact between diamond particles and the HEA, which contains elements such as Fe, Co, and Ni that promote diamond graphitization, effectively inhibits the transformation to graphite, even at a temperature of 1000°C.

In the initial stage of abrasion, corresponding to the stage of significant fluctuations in the friction coefficient, the abrasion loss of Si_3N_4 balls constitutes the majority of the overall wear test. Both the FeNiCrCuAl HEA matrix and the Si_3N_4 balls presented a rapid loss of mass during this period. Following the wear adaptation stage, the wear was predominantly attributed to diamond particles that gradually protruded from the composite material. The effect of the FeNiCrCuAl HEA matrix in this stage was primarily to support and retain the diamond particles. The TiC coating encircled the diamond particles helped maintain their complete crystal structure during the sintering process, thereby preserving optimal cutting conditions. Meanwhile, the TiC coating was the first to be abraded during the contact between the diamond particles and the Si_3N_4 ball friction pair, ensuring that the diamond particles sustained excellent cutting conditions for an extended duration.

Diamond particles aren't observed detaching from the abrasion surface of the composites after wear experiments. The TiC coating encircled the diamond surface, serving as the transition from diamond interface to FeNiCrCuAl HEA matrix, providing a strong interface bonding between the diamond and the FeNiCrCuAl HEA, significantly enhancing FeNiCrCuAl HEA matrix's ability to retain diamond particles. The cutting property of the composites improved with an increase in the diamond mass fraction at lower diamond contents. However, when the diamond mass fraction reached 12 wt.%, the cutting property of the composites on Si_3N_4 balls presented a significant decrease. This decline may be attributed to the increased density of diamond particles in the composites, which affected the cutting depth of individual diamond particles on the Si_3N_4 balls, resulting in a reduced abrasion area on the Si_3N_4 balls. Significant cutting depths were observed on the Si_3N_4 balls corresponding to samples D3, D5, and D7, due to the relative sliding between the Si_3N_4 balls and the diamond particles during friction. Parallel groove scratches of various depths were observed, exhibiting an abrasive wear mechanism on the abrasion surface. Pits formed by localized spalling could be observed in the friction morphology of the Si_3N_4 balls corresponding to sample D12. The reason was that the high density of diamond particles in sample D12 reduced the cutting depth on the Si_3N_4 balls. However, the frequency of impacts caused by diamond particles on the abrasion surface of the Si_3N_4 balls increased significantly over a limited time. The surface of the Si_3N_4 balls sustained continuous impacts from diamond particles during friction, ultimately leading to the formation of pitting. These pits interconnected eventually and resulted in localized spalling morphology.

4. Conclusion

FeNiCrCuAl HEA/Diamond composites with diamond mass fractions of 3 wt.%, 5 wt.%, 7 wt.%, and 12 wt.% were successfully prepared by the SPS process. All of the samples achieved a densification test by Archimedes' drainage method of over 96 % and exhibited excellent wear resistance, and the 7 wt.% diamond composite sample presented the best wear performance.

The mechanical properties of the composites primarily depend on the mass fraction of diamond added to the FeNiCrCuAl HEA. The density of the composites gradually decreases as the mass fraction of diamond increases. Specifically, when the mass fraction of diamond rises from 0 wt.% to 12 wt.%, the density of the composites decreases from 7.25 g/cm^3 to 6.44 g/cm^3. Concurrently, the hardness of the FeNiCrCuAl HEA matrix within the composites increases from 432.4 $HV_{0.5}$ to 500.2 $HV_{0.5}$. The primary reason for the increased hardness of the HEAs matrix is the diffusion of TiC from the diamond surface into the HEAs matrix, as well as the lattice distortion caused by the diffusion of Ti and C atoms into the FeNiCrCuAl HEA matrix.

The results of the three-point bending experiment results indicated that the flexural strength of the composites decreases as the mass fraction of diamond added to the FeNiCrCuAl HEA matrix increases. Specifically, when the mass fraction of diamond

in the composites increased from 3 wt.% to 12 wt.%, the flexural strength decreased from 499.4 MPa to 277.0 MPa. The addition of diamond into the HEAs creates heterogeneous interfaces within the FeNiCrCuAl HEA structure. Although the TiC coating on the surface of the diamond fills the gaps between the diamond and the HEAs to promote strong bonding, its bonding strength remains lower than that of the intrinsic bonding within the HEA matrix. The presence of numerous heterogeneous interfaces significantly contributes to a significant reduction in bending strength.

All of the diamond composites exhibited abrasive wear during the friction and wear experiments. The detachment of hard phases, such as TiC absorbed on the diamond surface, caused abrasion scratches to extend from the diamond particles in the direction of friction. At the same time, lamellar peeling occurred in the localized stress concentration areas of the friction surface. The abrasion area of Si_3N_4 ball friction pair reflected the wear resistance of the diamond composites. The Si_3N_4 ball corresponding to 7 wt.% diamond composite sample exhibited the largest abrasion area, indicating that the D7 sample has the best wear resistance, which is consistent with the wear resistance suggested by the average friction coefficient. FeNiCrCuAl HEA/Diamond composites exhibit excellent hardness and wear resistance. However, an increase in the mass fraction of diamond will reduce the flexural strength of the composites. The composites with 5 wt.% and 7 wt.% diamond addition have similar hardness and wear resistance. The hardness of the composite sample D5 is 449.9 $HV_{0.5}$, and the average friction coefficient is 0.17. While the hardness of the sample D7 is 458.2 $HV_{0.5}$, and the average friction coefficient is 0.16. When comparing the flexural strength of the composites, the flexural strength of D5 is 410.0 MPa, which is approximately 28.5% higher than that of the D7 sample, and only 17.9% lower than that of the D3 sample. Taking into comprehensive consideration the hardness, wear resistance, and flexural strength of the diamond/FeNiCrCuAl HEA composites, as well as their grinding ability on Si_3N_4 balls, the composite material with 5 wt.% diamond addition is more suitable for application in diamond grinding tools.

In this work, techniques such as SEM and XRD were employed to characterize the microstructure and phase composition of the composites. Additionally, the mechanical properties of the composites, including hardness, density, wear resistance, and flexural strength were tested. However, there are still certain deficiencies in the exploration of the properties of FeNiCrCuAl HEA/diamond composites. The research lacks investigations into aspects such as thermal stability under cyclic loading, corrosion resistance, and long-term performance. In future work, further studies will be conducted on the above-mentioned properties to provide a sufficient scientific basis for the application of FeNiCrCuAl HEA in diamond tool materials.

Acknowledgments

This work was supported by the Henan Province Science and Technology Research Project (252102221051, 252102231020, 242102321102), Key Scientific Research Projects of Henan Province (25A510001), International Science and Technology Cooperation Project of Henan Province (242102520005), General Project of Education Science Planning in Henan Province (2024YB0516), Nanyang Basic and Frontier Technology Research Special Project (23JCQY2022), and Research Project of Higher Education Teaching Reform of China Textile Industry Federation (2021BKJGLX529, 2021BKJGLX530).

REFERENCES

[1] J.W. Yeh, S.K. Chen, S.J. Lin, J.Y. Gan, T.S. Chin, T.T. Shun, C.H. Tsau, S.Y. Chang, Nanostructured high-entropy alloys with multiple principal elements: novel alloy design concepts and outcomes. Adv. Eng. Mater. **6** (5), 299-303 (2004).
DOI: https://doi.org/10.1002/adem.200300567

[1] A. Verma, P. Tarate, A.C. Abhyankar, M.R. Mohape, D.S. Gowtam, V.P. Deshmukh, T. Shanmugasundaram, High temperature wear in $CoCrFeNiCu_x$ high entropy alloys: The role of Cu. Scr. Mater. **161**, 28-31 (2019).
DOI: https://doi.org/10.1016/j.scriptamat.2018.10.007

[23] M. Ma, C. Zhu, Z. Wang, Y. Dong, L. Ding, H. Ma, Y. Xi, B. Wang, D. Zhu, D. Zhang, Microstructure and wear and corrosion resistance of $CoCrFeMoNiSi_x$ (x = 0.25, 0.50, 0.75) HEACs prepared by plasma cladding. Crystals **15** (2), 123 (2025).
DOI: https://doi.org/10.3390/cryst15020123

[4] E.P. George, W.A. Curtin, C.C. Tasan, High entropy alloys: A focused review of mechanical properties and deformation mechanisms. Acta Mater. **188**, 435-474 (2020).
DOI: https://doi.org/10.1016/j.actamat.2019.12.015

[5] T.T. Shun, L.Y. Chang, M.H. Shiu, Microstructures and mechanical properties of multi-principal component $CoCrFeNiTi_x$ alloys. Mater. Sci. Eng. A **556**, 170-174 (2012).
DOI: https://doi.org/10.1016/j.msea.2012.06.075

[6] W.R. Wang, W.L. Wang, J.W. Yeh, Phases, microstructure and mechanical properties of $Al_xCoCrFeNi$ high-entropy alloys at elevated temperatures. J. Alloys Compd. **589**, 143-152 (2014).
DOI: https://doi.org/10.1016/j.jallcom.2013.11.084

[7] M. Ma, Z. Wang, C. Zhu, Y. Dong, L. Zhao, L. Liu, D. Zhu, D. Zhang, Microstructure and wear behavior of $Al_xCoCuNiTi$ (x = 0, 0.4, and 1) high-entropy alloy coatings. Metals **14** (11), 1280 (2024).
DOI: https://doi.org/10.3390/met14111280

[8] T.T. Shun, L.Y. Chang, M.H. Shiu, Microstructure and mechanical properties of multi-principal component $CoCrFeNiMo_x$ alloys. Mater. Charact. **70**, 63-67 (2012).
DOI: https://doi.org/10.1016/j.matchar.2012.05.005

[9] F. Otto, A. Dlouhý, C. Somsen, H. Bei, G. Eggeler, E.P. George, The influences of temperature and microstructure on the tensile properties of a CoCrFeMnNi high-entropy alloy. Acta Mater. **61** (15), 5743-5755 (2013).
DOI: https://doi.org/10.1016/j.actamat.2013.06.018

[10] D.B. Miracle, O.N. Senkov, A critical review of high entropy alloys and related concepts. Acta Mater. **122**, 448-511 (2017).
DOI: https://doi.org/10.1016/j.actamat.2016.08.081

[11] M. Ma, Z. Wang, C. Zhu, Y. Dong, L. Liu, L. Zhao, Q. Cui, D. Zhu, D. Zhang, Effect of Mn doping on microstructure and corrosion behavior of CoCuNiTi high-entropy alloy coatings. Crystals **15** (1), 29 (2025). DOI: https://doi.org/10.3390/cryst15010029

[12] D. Kumar, Recent advances in tribology of high entropy alloys: A critical review. Prog. Mater. Sci. **136**, 101106 (2023). DOI: https://doi.org/10.1016/j.pmatsci.2023.101106

[13] C.A. Huang, C.H. Shen, W.Z. Huang, J.S. Lo, P.L. Lai, Grinding performance of electroplated diamond tools strengthened with Cr-C deposit using D-150 diamond particles. Int. J. Adv. Manuf. Technol. **121** (7), 4549-4558 (2022). DOI: https://doi.org/10.1007/s00170-022-09604-3

[14] B. Xiao, H.J. Xu, Y.C. Fu, J.H. Xu, Form and distribution characterization of reaction products at the brazing interface between Ni-Cr alloy and diamond. Key Eng. Mater. **259**, 151-153 (2004). DOI: https://doi.org/10.4028/www.scientific.net/KEM.259-260.151

[15] Y. Zhang, T. Han, M. Xiao, Y. Shen, Preparation of diamond reinforced $NiCoCrTi_{0.5}Nb_{0.5}$ high-entropy alloy coating by laser cladding: microstructure and wear behavior. J. Therm. Spray Technol. **29**, 1827-1837 (2020). DOI: https://doi.org/10.1007/s11666-020-01067-w

[16] Y. Zhang, T. Han, M. Xiao, Y. Shen, Tribological behavior of diamond reinforced $FeNiCoCrTi_{0.5}$ carbonized high-entropy alloy coating. Surf. Coat. Technol. **401**, 126233 (2020). DOI: https://doi.org/10.1016/j.surfcoat.2020.126233

[17] F. Bu, C. Li, C. Shen, X. Zhang, X. Sun, X. Feng, Microstructures and wear resistance of diamond-reinforced $FeCoCrNiAl_{0.5}Ti_{0.5}Si_{0.2}$-carbonized high-entropy alloy coatings by laser cladding. Trans. Indian Inst. Met. **75** (8), 1967-1978 (2022). DOI: https://doi.org/10.1007/s12666-022-02580-y

[18] H. Wang, W. Zhang, Y. Peng, M. Zhang, S. Liu, Y. Liu, Microstructures and wear resistance of FeCoCrNi-Mo high entropy alloy/diamond composite coatings by high-speed laser cladding. Coatings **10** (3), 300 (2020). DOI: https://doi.org/10.3390/coatings10030300

[19] Z. Zhang, J. Zhang, M. Zhang, P. Peng, First-principles calculations on brazed diamond with FeCoCrNi high entropy alloys doped with strong carbide-forming elements. Solid State Commun. **357**, 114980 (2022). DOI: https://doi.org/10.1016/j.ssc.2022.114980

[20] W. Zhang, M.Y. Zhang, Y.B. Peng, L. Wang, Y. Liu, S. Hu, Y. Hu, Interfacial structures and mechanical properties of a high entropy alloy-diamond composite. Int. J. Refract. Met. Hard Mater. **86**, 105109 (2020). DOI: https://doi.org/10.1016/j.ijrmhm.2019.105109

[21] N. Razumov, T. Makhmutov, A. Kim, B. Shemyakinsky, A. Shakhmatov, V. Popovich, A. Popovich, Refractory CrMoNbWV high-entropy alloy manufactured by mechanical alloying and spark plasma sintering: evolution of microstructure and properties. Materials **14** (3), 621 (2021). DOI: https://doi.org/10.3390/ma14030621

[22] G. Buluc, I. Florea, O. Bălţătescu, C. Roman, I. Carcea, Microstructure and mechanical properties of FeNiCrCuAl high entropy alloys. Adv. Mater. Res. **1036**, 101-105 (2014). DOI: https://doi.org/10.4028/www.scientific.net/AMR.1036.101

[23] Q. Zhao, X. Huang, Z. Zhan, S. Zhou, X. He, H. Huang, P. Zhu, L. Wei, X. Li, Y. Xie, Effect of exposure temperature on the corrosion behavior of a FeNiCrCuAl high entropy alloy in supercritical water. Corros. Sci. **227**, 111755 (2024). DOI: https://doi.org/10.1016/j.corsci.2023.111755

[24] C. Du, L. Hu, X. Ren, Y. Li, F. Zhang, P. Liu, Y. Li, Cracking mechanism of brittle FeCoNiCrAl HEA coating using extreme high-speed laser cladding. Surf. Coat. Technol. **424**, 127617 (2021). DOI: https://doi.org/10.1016/j.surfcoat.2021.127617

[25] J.C. Arnault, Nano-diamonds: Advanced Material Analysis, Properties and Applications. 2017 Elsevier, Micro Nano Technol., Edition.

[26] D. Zhang, G. Zhang, H. Yu, W. Lv, K. Wen, H. Xu, Controlling interfacial composition and improvement in bonding strength of compound casted Al/steel bimetal via Cr interlayer. J. Mater. Res. Technol. **23**, 4385-4395 (2023). DOI: https://doi.org/10.1016/j.jmrt.2023.02.053

[27] R. Tian, C. Hang, Y. Tian, J. Feng, Brittle fracture induced by phase transformation of Ni-Cu-Sn intermetallic compounds in Sn-3Ag-0.5Cu/Ni solder joints under extreme temperature environment. J. Alloys Compd. **777**, 463-471 (2019). DOI: https://doi.org/10.1016/j.jallcom.2018.10.394

[28] A. Wierzbicka-Miernik, K. Miernik, J. Wojewoda-Budka, L. Litynska-Dobrzynska, G. Garzel, Microstructure and chemical characterization of the intermetallic phases in Cu/ (Sn, Ni) diffusion couples with various Ni additions. Intermetallics **59**, 23-31 (2015). DOI: https://doi.org/10.1016/j.intermet.2014.12.001

[29] C. Sang, X. Cai, L. Zhu, X. Ren, G. Niu, X. Wang, P. Feng, Interfacial microstructure of Ti/Ni joints with Ti–Al interlayer by rapid thermal explosion bonding in vacuum. Vacuum **171**, 109028 (2020). DOI: https://doi.org/10.1016/j.vacuum.2019.109028

[30] M.I. De Barros, D. Rats, L. Vandenbulcke, G. Farges, Influence of internal diffusion barriers on carbon diffusion in pure titanium and Ti-6Al-4V during diamond deposition. Diam. Relat. Mater. **8**, 1022-1032 (1999). DOI: https://doi.org/10.1016/s0925-9635(98)00439-7

[31] X.Y. Liu, W.G. Wang, D. Wang, D.R. Ni, L.Q. Chen, Z.Y. Ma, Effect of nanometer TiC coated diamond on the strength and thermal conductivity of diamond/Al composites. Mater. Chem. Phys. **182**, 256-262 (2016). DOI: https://doi.org/10.1016/j.matchemphys.2016.07.030

[32] W. Zhang, M. Zhang, Y. Peng, F. Liu, Y. Liu, S. Hu, Y. Hu, Effect of Ti/Ni coating of diamond particles on microstructure and properties of high-entropy alloy/diamond composites. Entropy **21** (2), 164 (2019). DOI: https://doi.org/10.3390/e21020164

[33] S.A. Agrawal, Simplified measurement of density of irregular shaped composites material using Archimedes principle by mixing two fluids having different densities. Int. Res. J. Eng. Technol. **8** (3), 1005-1009 (2021).

[34] H. Wang, W. Zhang, Y. Peng, M. Zhang, S. Liu, Y. Liu, Microstructures and wear resistance of FeCoCrNi-Mo high entropy alloy/diamond composite coatings by high-speed laser cladding. Coatings **10** (3), 300 (2020). DOI: https://doi.org/10.3390/coatings10030300

[35] Y. Zhang, T. Han, M. Xiao, Y. Shen, Preparation of diamond reinforced $NiCoCrTi_{0.5}Nb_{0.5}$ high-entropy alloy coating by laser cladding: microstructure and wear behavior. J. Therm. Spray Technol. **29**, 1827-1837 (2020).
DOI: https://doi.org/10.1007/s11666-020-01067-w

[36] X.Y. Ning, Study on preparation of oxide dispersion strengthened copper alloy and application in diamond tools. Master thesis, General Research Institution for Nonferrous Metals, Beijing, 100006, May.

[37] M. Zhang, W. Zhang, Y. Liu, B. Liu, J. Wang, FeCoCrNiMo high-entropy alloys prepared by powder metallurgy processing for diamond tool applications. Powder Metall. **61** (2), 123-130 (2018). DOI: https://doi.org/10.1080/00325899.2018.1429044

[38] P.A. Loginov, A.D. Fedotov, S.K. Mukanov, O.S. Manakova, A.A. Zaitsev, A.S. Akhmetov, S.I. Rupasov, E.A. Levashov, Manufacturing of metal–diamond compositeswith high-strength CoCr-Cu_xFeNi high-entropy alloy used as a binder. Materials **16** (3), 1285(2023). DOI: https://doi.org/10.3390/ma16031285

[39] C. Timmer, W. Tillmann, L. Wojarski, M.P. Ferreira, Investigation of the applicability of Cu–Fe–Mn–Ni based high entropy and compositionally complex alloys as metal matrix composites for cobalt-free hot-pressed diamond tools. J. Mater. Res. Technol. **26**, 5518-5534 (2023).
`DOI: https://doi.org/10.1016/j.jmrt.2023.08.272

[40] Y. Zhang, T. Han, M. Xiao, Y. Shen, Tribological behavior of diamond reinforced $FeNiCoCrTi_{0.5}$ carbonized high-entropy alloy coating. Surf. Coat. Technol. **401**, 126233 (2020).
DOI: https://doi.org/10.1016/j.surfcoat.2020.126233

[41] J.K. Park, W.S. Lee, Y.J. Baik, Grain size refinement of the diamond film deposited on the WC–Co cutting inserts using direct current biasing. Surf. Coat. Technol. **171** (1-3), 1-5 (2003).
DOI: https://doi.org/10.1016/s0257-8972(03)00226-3

[42] C. Artini, M.L. Muolo, A. Passerone, Diamond-metal interfaces in cutting tools: a review. J. Mater. Sci. **47** (7), 3252-3264 (2012).
DOI: https://doi.org/10.1007/s10853-011-6164-6

[43] Y. Peng, Y. Kong, W. Zhang, M. Zhang, H. Wang, Effect of diffusion barrier and interfacial strengthening on the interface behavior between high entropy alloy and diamond. J. Alloys Compd. **852**, 157023 (2021).
DOI: https://doi.org/10.1016/j.jallcom.2020.157023

[44] Y. Geng, J. Chen, H. Tan, J. Chen, S. Zhu, J. Yang, Tribological performances of CoCrFeNiAl high entropy alloy matrix solid-lubricating composites over a wide temperature range. Tribol. Int. **157**, 106912 (2021).
DOI: https://doi.org/10.1016/j.triboint.2021.106912

[45] W. Zhang, M. Zhang, Y. Peng, F. Liu, Y. Liu, S. Hu, Y. Hu, Effect of Ti/Ni coating of diamond particles on microstructure and properties of high-entropy alloy/diamond composites. Entropy **21** (2), 164 (2019).
DOI: https://doi.org/10.3390/e21020164

[46] Q. Gu, J. Peng, L. Xu, C. Srinivasakannan, L. Zhang, Y. Xia, Q. Wu, H. Xia, Preparation of Ti-coated diamond particles by microwave heating. Appl. Surf. Sci. **390**, 909-916 (2016).
DOI: https://doi.org/10.1016/j.apsusc.2016.08.168